DENSE-HAZE: A BENCHMARK FOR IMAGE DEHAZING WITH DENSE-HAZE AND HAZE-FREE IMAGES

Codruta O. Ancuti [*], *Cosmin Ancuti* [*†], *Mateu Sbert*[†], *Radu Timofte*[‡]

[*] ETcTI, Universitatea Politehnica Timisoara, Romania
[†] Institute of Informatics and Applications, University of Girona, Spain
[‡] CVL, ETH Zurich, Switzerland

ABSTRACT

Single image dehazing is an ill-posed problem that has recently drawn important attention. Despite the significant increase in interest shown for dehazing over the past few years, the validation of the dehazing methods remains largely unsatisfactory, due to the lack of pairs of real hazy and corresponding haze-free reference images. To address this limitation, we introduce **Dense-Haze** – a novel dehazing dataset. Characterized by dense and homogeneous hazy scenes, **Dense-Haze** contains 33 pairs of real hazy and corresponding haze-free images of various outdoor scenes. The hazy scenes have been recorded by introducing real haze, generated by professional haze machines. The hazy and haze-free corresponding scenes contain the same visual content captured under the same illumination parameters. **Dense-Haze** dataset aims to push significantly the state-of-the-art in single-image dehazing by promoting robust methods for real and various hazy scenes. We also provide a comprehensive qualitative and quantitative evaluation of state-of-the-art single image dehazing techniques based on the **Dense-Haze** dataset. Not surprisingly, our study reveals that the existing dehazing techniques perform poorly for dense homogeneous hazy scenes and that there is still much room for improvement.

I. INTRODUCTION

Haze represents one of the atmospheric phenomena most challenging for camera sensors and vision applications. Haze is an often occurring meteorological phenomenon especially during autumn and spring in temperate climates being generated by particles that scatter and absorb the incident light. The visibility of such hazy scene is highly degraded and as a result they are characterized by poor contrast, and additional noise. For instance, the presence of haze has a great impact in the road traffic as it may severely reduce the visibility for drivers. As a result, restoring the contents in hazy images – process known as *dehazing* – is important for several outdoor image processing and computer vision applications such as ADAS, remote sensing and visual surveillance.

Restoring the visibility in hazy images based only on a single input RGB image is challenging, being a mathematically ill-posed problem [1], [2], [3], [4], [5], [6], [7], [8], [9], [10]. The problem is related also to underwater image dehazing [11], [12], [13], [14]. Fattal [1] introduces a Markov Random Field (MRF) method assuming that shading and transmission functions are locally statistically uncorrelated. He et al. [5] propose the Dark Channel Prior (DCP), a simple but effective solution to estimate the transmission map. Instead of using alpha-matting as in [5], the method of Meng et al. [15] is based on a regularization strategy and refines the boundaries of the rough transmission estimated by DCP. Berman et al. [16] extends the model proposed in [17] observing

Fig. 1. *Three examples of the **Dense-Haze** dataset that provides* 33 *pairs of hazy and corresponding haze-free (groundtruth) outdoor images.*

that the RGB color space can be approximated by a discrete set of color clusters. Another category is represented by multi-scale fusion approaches [18], [19] that enhance the hazy scenes without explicitly estimating the transmission map. More recently, several machine learning dehazing methods [20], [21], [22], [23], [24], [25], [26] have been introduced in the literature. DehazeNet [21] is trained based on a synthetically built dehazing dataset to estimate the transmission map which is subsequently used to compute a haze-free image via traditional optical model. Employing also a synthesized dataset in the training stage, Ren et al. [22] define a coarse-to-fine neural network consisting of a cascade of CNN layers.

Although the interest shown for the image dehazing problem has increased significantly over the past few years, the validation of the proposed dehazing methods [27] has generally remained unmet, mainly due to the absence of ground-truth (haze-free) images. Recording realistic images is very challenging and time-consuming due to the practical issues associated to the recording of reference and hazy images under identical illumination conditions. As a result, most of the existing dehazing assessment datasets [28], [29], [30] rely on synthesized hazy images using a simplified optical model and known depth. Tarel et al. [28] introduced the first synthetic dehazing dataset (FRIDA) which contains 66 computer graphics generated traffic scenes. D-HAZY [29] is another synthetic dehazing dataset with 1400+ real images and corresponding depth maps used to synthesize hazy scenes based on Koschmieder's light propagation model [31]. The dataset of Luthen et al. [32] contains only four sets of indoor scenes considering NIR images as ground-truth.

So far the focus in the dehazing literature has been on relatively

light hazy conditions which potentially limits the utility of the proposed existing dehazing techniques for real scenes with dense haze. The introduction of a dehazing dataset with dense haze and corresponding haze-free reference images is very important to assess the existing dehazing techniques and furthermore to advance the research in the dehazing field.

The main contribution of this paper is **Dense-Haze**, a new realistic dehazing dataset. Characterized by dense and homogeneous hazy scenes, **Dense-Haze** contains 33 pairs of real hazy and corresponding haze-free images of various outdoor scenes. In order to generate hazy scenes we used a professional haze machine that imitates real haze with high fidelity. To preserve the illumination conditions, all the outdoor scenes are static and have been recorded during cloudy days. Basically, **Dense-Haze** extends the O-HAZE [33] dataset that has been used recently for the first single image dehazing challenge ever organized [34]. In contrast to O-HAZE that contains only light hazy scenes, **Dense-Haze** is more challenging since all the recorded scenes contain a denser and more homogeneous haze layer (see Fig. 1). We believe that introducing the **Dense-Haze** dataset will push significantly the state-of-the-art in single-image dehazing methods making them to be more robust for real and various dense haze scenes.

A second contribution of this paper is a comprehensive qualitative and quantitative evaluation of the state-of-the-art single image dehazing techniques based on the **Dense-Haze** dataset. In our study we compare a set of representative dehazing methods and evaluate them using traditional measures such as PSNR and SSIM on **Dense-Haze** dataset. Our experimental results reveal that the existing dehazing techniques perform poorly for dense hazy scenes, which was somewhat expected given the fact the most of the existing methods were introduced and validated on lighter haze conditions. There is clearly much room for improvement and our proposed **Dense-Haze** dataset can promote and benchmark research for robust image dehazing solutions.

II. RECORDING DENSE-HAZE DATASET

In this section we discuss the methodology of recording the 33 pairs of hazy and haze-free (ground-truth) outdoor images of the **Dense-Haze** dataset. As we briefly discussed, a crucial problem in collecting such images is represented by capturing pixel-level images for each scene, with and without, haze under identical conditions, using the same camera settings, viewpoint, etc. Besides assuring that the scene is static, the scene components keep do not change their spatial position during the recording (quite challenging for natural scenes due to numerous factors), the most challenging issue is to preserve the outdoor scene illumination.

Therefore, the outdoor scenes have been recorded in general during in the morning of cloudy days. Additionally, another important constraint was given by the influence of the wind. In order to limit fast spreading of the haze in the scene we could record images only when the wind speed was below 2-3 km/h. This constraint was hard to meet, it is a main reason for the 8 weeks duration required by the recording of the 33 outdoor scenes from **Dense-Haze**.

To yield hazy scenes, the haze was spread using two professional haze machines (LSM1500 PRO 1500 W), which generate vapor particles with diameter size (typically 1 - 10 microns) similar to the particles of the atmospheric haze. The haze machines use cast or platen type aluminum heat exchangers to induce liquid evaporation. In order to simulate the effect occurring with water haze over larger distances than the investigated 20-30 meters, we used special (haze) liquid with higher density. To obtain a dense and homogeneous haze layer in the scene, we employed for 2-3 minutes both haze machines powered by a portable 2800 Watt generator, and waited for another 2-3 minutes.

Before introducing haze in the scenes, we settled the recording setup composed by a tripod and a Sony A5000 camera that was remotely controlled (Sony RM-VPR1). This setup allowed to acquire JPG and ARW (RAW) 5456×3632 images, with 24 bit depth. For each scene recording a manual adjustment of the camera settings has been performed. We use the same camera setting to capture the haze-free and hazy images of the same scene. Basically, the camera parameters related to the shutter-speed (exposure-time), the aperture (F-stop), the ISO and white-balance have been kept identical when recording hazy and haze-free scenes. Therefore, the closer regions (that in general are less distorted by haze) have similar appearance (in terms of color) in the corresponding scenes.

The optimal camera parameters (aperture-exposure-ISO), have been set based on the built-in light-meter of the camera, but also using an external exponometer (Sekonic). For the custom white-balance, we used the middle gray card (18% gray) of the color checker. This is a common photographic process that requires to use the camera white-balance mode in manual mode and place the reference gray-card in the front of the camera (the gray-card was placed in the center of the scene in the range of four meters). Additionally, all the recorded scenes contain a color checker to allow for the post-processing of the recorded images. We used a classical Macbeth color checker with the size 11 by 8.25 inches with 24 squares of painted samples (4×6 grid).

III. EVALUATED DEHAZING TECHNIQUES

In this work we evaluate qualitatively and quantitatively several state-of-the-art single image dehazing techniques based on the **Dense-Haze** dataset. For the sake of completeness, in the following paragraphs we briefly review the evaluated dehazing methods.

He et al. [5], introduce probably the most influential single-image dehazing approach. The authors of [5] define the Dark Channel Prior (DCP), a statistic observation that yields a rough estimate (per patch) of the transmission map. DCP is a heuristic approach that builds on the observation that excepting the sky/hazy regions the local regions contain pixels that present low intensity in at least one of the color channels. The roughly estimated transmission is refined by an alpha matting strategy [5] or by using guided filter [36]. In our evaluation, the results of **He et al.** [5] have been generated using the DCP refined with guided filters.

Meng et al. [15] introduce a method that builds on the DCP [5]. The estimated transmission map (based on DCP) is refined further using a boundary constraint that is combined with a weighted L1 norm regularization. Overall, this method mitigates the lack of resolution in the DCP transmission map. Moreover, the method of Meng et al. [15] demonstrates some improvement compared with the He et al. [5] technique.

Fattal [17] makes use of color-lines in the RGB color space firstly introduced by Omer et al. [37]. The method is built on the

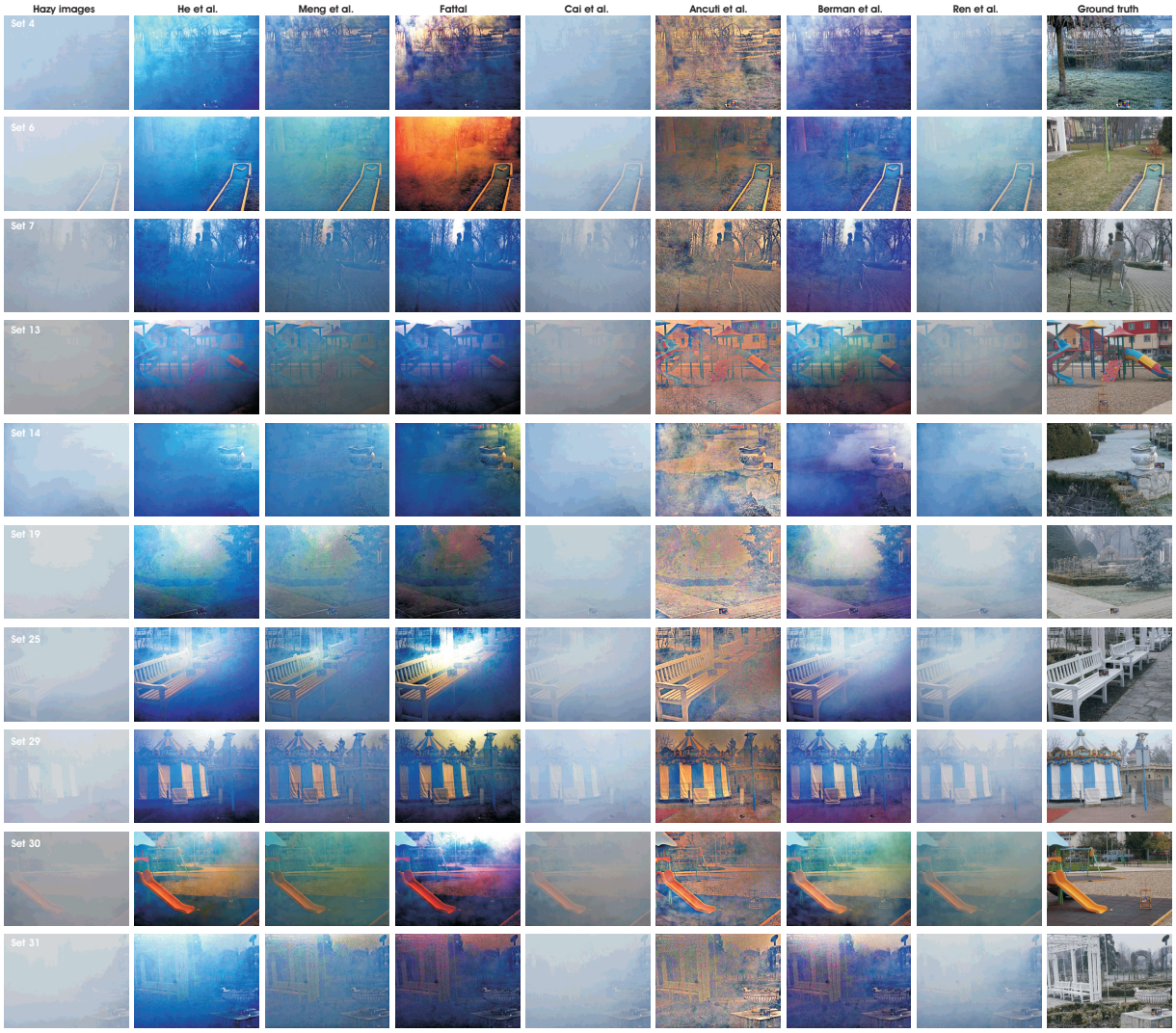

Fig. 2. ***Comparative results of representative single image dehazing techniques.*** *The first column shows the hazy images and the last column shows the ground truth. The middle columns, from left to right, present the results of He et al. [5], Meng et al. [15], Fattal [17], Cai et al. [21], Ancuti et al. [35], Berman et al. [16] and Ren et al. [22].*

observation that the distributions of pixels in small natural image patches exhibit one-dimensional structures. This finding allows to compute a rough estimate of the transmission map that is further refined by employing a Markov Random Field model that filters the noise and removes some artifacts due to the scattering.

Cai et al. [21] introduces **DehazeNet**, a convolutional neural network (CNN) approach that trains a model to map hazy to haze-free patches. **DehazeNet** first extracts the features extraction, than employs a multi-scale mapping and finally a non-linear regression is performed. The model is trained using a synthesized dehazing dataset.

Ancuti et al. [35] rely also on DCP, but their work the authors introduce a simple method to estimate locally the airlight constant. Deriving several input images obtained from distinct definitions of the locality notion, the method employs a multi-scale fusion strategy. Designed initially as a solution for more complex night-time hazy scenes (that are characterized by severe scattering and multiple sources of light), this fusion-based strategy shown to be competitive also for day-time single-image dehazing.

Berman et al. [16] extends the color-lines concept of [17] observing that the RGB color space can be approximated by a discrete set of color clusters. The method builds on the observation that the pixels of a cluster appear in the entire image plane. As a result, the pixels in a cluster are affected differently by the haze and convey information that can be used to estimate the transmission map.

Ren et al. [22] is also a a convolutional neural network (CNN) strategy, but different than [21], they first estimate the transmission map by a coarse-scale network, that is subsequently refined by a fine-scale network. Similarly, the training of the network is

	He et al. [5]		**Meng et al.** [15]		**Fattal** [17]		**Cai et al.** [21]		**Ancuti et al.** [35]		**Berman** [16]		**Ren et al.** [22]	
	PSNR	CIEDE2000	PSNR	CIEDE2000	PSNR	CIEDE2000	PSNR	CIEDE2000	PSNR	CIEDE2000	PSNR	CIEDE2000	PSNR	CIEDE2000
Set 4	14.12	21.54	14.57	21.22	11.10	27.98	10.08	28.50	14.39	24.89	12.55	26.08	11.39	25.04
Set 6	15.99	30.19	15.47	27.43	12.32	33.31	10.97	30.40	15.74	19.51	14.79	34.92	12.46	28.05
Set 7	15.65	22.23	16.97	21.13	14.59	26.84	13.95	20.30	18.48	17.07	15.29	26.80	16.45	18.66
Set 13	13.43	24.04	15.03	21.85	11.64	30.74	14.54	19.50	17.57	19.84	12.98	25.85	15.34	18.88
Set 14	15.06	24.63	14.67	24.40	13.11	27.08	9.58	30.00	11.18	28.31	12.62	28.02	11.78	25.59
Set 19	14.42	20.27	13.92	22.08	10.71	27.24	11.09	24.44	13.27	24.52	12.24	24.84	11.29	23.35
Set 25	14.51	19.88	14.78	20.72	11.54	26.28	11.20	22.06	15.62	21.00	11.60	24.89	12.29	20.06
Set 29	14.36	19.72	14.86	19.53	11.06	28.15	14.00	18.06	14.77	19.08	13.99	22.85	16.00	14.85
Set 30	14.69	19.78	15.12	23.23	10.48	33.03	13.45	20.13	16.24	20.72	13.72	22.47	14.58	20.55
Set 31	14.22	21.79	14.60	21.19	9.88	32.66	11.61	22.11	13.98	21.99	13.03	25.43	12.52	20.59

Table I. ***Quantitative evaluation.*** *In this table are presented 10 randomly picked up sets from our* ***Dense-Haze*** *dataset (the hazy images, ground truth and the results are shown in Fig.2). Using the haze-free (ground-truth) images we can compute the PSNR and CIEDE2000 values for the dehazed images produced by the evaluated techniques.*

	He et al. [5]	**Meng et al.** [15]	**Fattal** [17]	**Cai et al.** [21]	**Ancuti et al.** [35]	**Berman et al.** [16]	**Ren et al.** [22]
SSIM	**0.398**	0.352	0.326	0.374	0.306	0.358	0.369
PSNR	14.557	**14.621**	12.114	11.362	13.669	13.176	12.524
CIEDE2000	**23.388**	23.420	27.834	26.879	24.417	27.918	24.689

Table II. Quantitative evaluation of the entire **Dense-Haze** dataset. This table presents the average values of the SSIM, PSNR and CIEDE2000 indexes, over the entire dataset (33 sets of images).

based on a synthetically generated dehazing dataset, obtained from haze-free images and their associated depth maps employed as a transmission map in the simplified optical model.

IV. EVALUATION AND DISCUSSION

The 33 pairs of hazy and haze-free (ground-truth) outdoor images of the **Dense-Haze** dataset have been used to evaluate several representative single image dehazing techniques that were briefly described in the previous section. In Fig.2 are shown 7 scenes of the **Dense-Haze** dataset and the dehazed image results generated using the methods of He et al. [5], Meng et al. [15], Fattal [17], Cai et al. [21], Ancuti et al. [35], Berman et al. [16] and Ren et al. [22].

By analyzing the visual results presented in Fig.2, we can observe that in general the DCP-based techniques [5], [15], [35] recover the global image structure. However, it can be observed that these methods , in general, distort the color in restored hazy regions. Such color shifting distortions are in general observable in the lighter regions. Similarly, the methods of Fattal [17] and Berman et al [16] introduce unpleasing color artifacts. Not surprisingly, although they do not introduce additional distortions, the learning-based approaches of Ren et al [22] and Cai et al [21], trained using synthetic hazy dataset, are not able to remove the hazy (white) appearance. Overall, Fig. 2 demonstrates that all the single image dehazing techniques from this study perform quite poorly for scenes from the **Dense-Haze** dataset. We conclude that the analyzed methods introduce structural distortions close to the sharp transitions with the artifacts more visible in regions far away from the camera. Moreover, in some cases the color distortions of the dehazed results look unnatural.

In addition to qualitative evaluation, **Dense-Haze** dataset makes possible for an objective quantitative evaluation of the single-image dehazing techniques. The haze-free (ground-truth) images available in our dataset allow to evaluate the quality of the corresponding dehazed results as a per-pixel fidelity to the ground-truth. In our evaluation, we considered the Peak Signal-to-Noise Ratio (PSNR), Structure Similarity Index Measure (SSIM) [38] and CIEDE2000 [39], [40]. While PSNR measures absolute errors, SSIM is a perception-based model that assesses results in the ranges in [-1,1], with maximum value 1 for two identical images. For color appearance, we consider CIEDE2000 [39], [40] that measures the color difference between two images and generates smaller values for better color preservation.

The quantitative results based on PSNR and CIEDE2000 of the image pairs shown in Fig. 2 are reported in Table I. Moreover, in Table III we summarize the overall quantitative results over the entire **Dense-Haze** dataset. From these tables, we can conclude that the He et al. [5] and Meng et al. [15] perform slightly better in terms of structure and color restoration compared with the other techniques. Overall, all analyzed dehazing methods achieve a relatively low performance in SSIM, PSNR and CIEDE2000 terms. This demonstrates once again the complexity of the image dehazing problem.

V. CONCLUSIONS

We introduce a novel dehazing dataset that contains dense-hazy scenes and their counterpart haze-free images. As revealed, by our proposed **Dense-Haze** dataset, the existing image dehazing techniques are not prepared to deal with dense hazy scenes and leaves significant room for improvement both qualitatively and quantitatively.

Acknowledgments: *Part of this work was supported by research grant GNaC2018 - ARUT, no. 1361-01.02.2019, financed by Politehnica University of Timisoara. Part of this work has was supported by 2020 European Union Research and Innovation Horizon 2020 under the grant agreement Marie Sklodowska-Curie No 712949 (TECNIOspring PLUS), as well as the Agency for the Competitiveness of the Company of the Generalitat de Catalunya - ACCIO: TECSPR17-1-0054 and also by Spanish project from Ministery of Economy and Competitivity, MINECO, TIN2016-75866-C3-3-R.*

VI. REFERENCES

[1] Raanan Fattal, "Single image dehazing," *SIGGRAPH*, 2008.

[2] Robby T. Tan, "Visibility in bad weather from a single image," *In IEEE Conference on Computer Vision and Pattern Recognition*, 2008.

[3] L. Kratz and K. Nishino, "Factorizing scene albedo and depth from a single foggy image," *ICCV*, 2009.

[4] J.-P. Tarel and N. Hautiere, "Fast visibility restoration from a single color or gray level image," *In IEEE ICCV*, 2009.

[5] K. He, J. Sun, and X. Tang, "Single image haze removal using dark channel prior," *In IEEE CVPR*, 2009.

[6] C. O. Ancuti, C. Ancuti, C. Hermans, and P. Bekaert, "A fast semi-inverse approach to detect and remove the haze from a single image," *ACCV*, 2010.

[7] C. O. Ancuti, C. Ancuti, and P. Bekaert, "Effective single-image dehazing by fusion," in *In IEEE ICIP*, 2010.

[8] C. Ancuti and C. O. Ancuti, "Effective contrast-based dehazing for robust image matching," *IEEE Geoscience and Remote Sensing Letters*, 2014.

[9] Q. Liu, X. Gao, L. He, and W. Lu, "Single image dehazing with depth-aware non-local total variation regularization," *IEEE Trans. Image Proc.*, 2018.

[10] C. O. Ancuti, C. Ancuti, and C. De Vleeschouwer, "Effective local airlight estimation for image dehazing," in *IEEE ICIP*, 2018.

[11] C. O. Ancuti, C. Ancuti, T. Haber, and P. Bekaert, "Fusion-based restoration of the underwater images," in *IEEE ICIP*, 2011.

[12] C. Ancuti, C. O. Ancuti, T. Haber, and P. Bekaert, "Enhancing underwater images and videos by fusion," in *IEEE Conference on Computer Vision and Pattern Recognition (CVPR)*, 2012.

[13] C. Ancuti, C. O. Ancuti, C. De Vleeschouwer, R. Garcia, and A.C. Bovik, "Multi-scale underwater descattering," in *ICPR*, 2016.

[14] C. O. Ancuti, C. Ancuti, C. De Vleeschouwer, and P. Bekaert, "Color balance and fusion for underwater image enhancement," in *IEEE Transactions on Image Processing*, 2018.

[15] G. Meng, Y. Wang, J. Duan, S. Xiang, and C. Pan, "Efficient image dehazing with boundary constraint and contextual regularization," *In IEEE Int. Conf. on Computer Vision*, 2013.

[16] D. Berman, T. Treibitz, and S. Avidan, "Non-local image dehazing," *IEEE Intl. Conf. Comp. Vision, and Pattern Recog*, 2016.

[17] Raanan Fattal, "Dehazing using color-lines," *ACM Trans. on Graph.*, 2014.

[18] C.O. Ancuti and C. Ancuti, "Single image dehazing by multi-scale fusion," *IEEE Transactions on Image Processing*, vol. 22(8), pp. 3271–3282, 2013.

[19] L. K. Choi, J. You, and A. C. Bovik, "Referenceless prediction of perceptual fog density and perceptual image defogging," *In IEEE Trans. on Image Processing*, 2015.

[20] K. Tang, J. Yang, and J. Wang, "Investigating haze-relevant features in a learning framework for image dehazing," *In IEEE Conference on Computer Vision and Pattern Recognition*, 2014.

[21] B. Cai, X. Xu, K. Jia, C. Qing, and D. Tao, "Dehazenet: An end-to-end system for single image haze removal," *IEEE Transactions on Image Processing*, 2016.

[22] W. Ren, S. Liu, H. Zhang, X. Cao J. Pan, and M.-H. Yang, "Single image dehazing via multi-scale convolutional neural networks," *Proc. European Conf. Computer Vision*, 2016.

[23] H. Zhang, V. Sindagi, and V. M. Patel, "Multi-scale single image dehazing using perceptual pyramid deep network," *IEEE CVPR*, 2018.

[24] S. Santra, R. Mondal, and B. Chanda, "Learning a patch quality comparator for single image dehazing," *IEEE Trans. Image Proc.*, 2018.

[25] R. Liu, L. Ma, Y. Wang, and L. Zhang, "Learning converged propagations with deep prior ensemble for image enhancement," *IEEE Trans. Image Proc.*, 2019.

[26] A. Wang, W. Wang, J. Liu, and N. Gu, "Aipnet: Image-to-image single image dehazing with atmospheric illumination prior," *IEEE Trans. Image Proc.*, 2019.

[27] Kede Ma, Wentao Liu, and Zhou Wang, "Perceptual evaluation of single image dehazing algorithms," in *IEEE ICIP*, 2015.

[28] J.-P. Tarel, N. Hautire, L. Caraffa, A. Cord, H. Halmaoui, and D. Gruyer, "Vision enhancement in homogeneous and heterogeneous fog," *IEEE Intelligent Transportation Systems Magazine*, 2012.

[29] C. Ancuti, C. O. Ancuti, and Christophe De Vleeschouwer, "D-hazy: A dataset to evaluate quantitatively dehazing algorithms," *IEEE ICIP*, 2016.

[30] Yanfu Zhang, Li Ding, and Gaurav Sharma, "Hazerd: an outdoor scene dataset and benchmark for single image dehazing," *IEEE ICIP*, 2017.

[31] H. Koschmieder, "Theorie der horizontalen sichtweite," in *Beitrage zur Physik der freien Atmosphare*, 1924.

[32] Julia Luthen, Julian Wormann, Martin Kleinsteuber, and Johannes Steurer, "A rgb/nir data set for evaluating dehazing algorithms," *Electronic Imaging*, 2017.

[33] C. O. Ancuti, C. Ancuti, C. De Vleeschouwer, and R. Timofte, "O-haze: a dehazing benchmark with real hazy and haze-free outdoor images," *IEEE CVPR, NTIRE Workshop*, 2018.

[34] C. Ancuti, C.O. Ancuti, R. Timofte, L. Van Gool, and L. Zhang et al., "Ntire 2018 challenge on image dehazing: Methods and results," *IEEE CVPR, NTIRE Workshop*, 2018.

[35] C. Ancuti, C. O. Ancuti, A.C. Bovik, and Christophe De Vleeschouwer, "Night time dehazing by fusion," *IEEE ICIP*, 2016.

[36] K. He, J. Sun, and X. Tang, "Guided image filtering," *In IEEE Transactions on Pattern Analysis and Machine Intelligence (TPAMI)*, 2013.

[37] I. Omer and M. Andwerman, "Color lines: image specific color representation," *In IEEE Conference on Computer Vision and Pattern Recognition*, 2004.

[38] Z. Wang, A. C. Bovik, H. R. Sheikh, and E. P. Simoncelli, "Image quality assessment: From error visibility to structural similarity," *IEEE Transactions on Image Processing*, 2004.

[39] G. Sharma, W. Wu, and E. Dalal, "The ciede2000 color-difference formula: Implementation notes, supplementary test data, and mathematical observations," *Color Research and Applications*, 2005.

[40] S. Westland, C. Ripamonti, and V. Cheung, "Computational colour science using matlab, 2nd edition," *Wiley*, 2012.